Ultramicroscopy 160 (2016) 247–251

Contents lists available at ScienceDirect

Ultramicroscopy

journal homepage: www.elsevier.com/locate/ultramic

Full length article

Simulation of the enhancement factor from an individual 3D hemisphere-on-post field emitter by using finite elements method

D.S. Roveri [a,*], G.M. Sant'Anna [a], H.H. Bertan [a], J.F. Mologni [b], M.A.R. Alves [a], E.S. Braga [a]

[a] Plasma Laboratory, Department of Semiconductors, Instrumentation and Photonics, School of Electric and Computer Engineering, University of Campinas (UNICAMP), Cidade Universitária Zeferino Vaz, P.O.Box 6101, Barão Geraldo, Campinas, 13083-852 São Paulo, Brazil
[b] ESSS-ANSYS, 423 Rocio St., ITC – International Trade Center, 10th Floor, Room 1001/1002, Vila Olímpia, 04552-000 São Paulo, Brazil

ARTICLE INFO

Article history:
Received 3 August 2015
Accepted 18 October 2015
Available online 28 October 2015

Keywords:
3D hemisphere-on-post
Field emitter
Enhancement factor
Anode positioning
Finite elements method

ABSTRACT

This paper presents a 3D computational framework for evaluating electrostatic properties of a single field emitter characterized by the hemisphere-on-post geometry. Numerical simulations employed the finite elements method by using Ansys-Maxwell software. Extensive parametric simulations were focused on the threshold distance from which the emitter field enhancement factor (γ) becomes independent from the anode-substrate gap (G). This investigation allowed demonstrating that the ratio between G and the emitter height (h) is a reliable reference for a broad range of emitter dimensions; furthermore, results permitted establishing $G/h \geq 2.2$ as the threshold condition for setting the anode without affecting γ.

1. Introduction

Field-effect electron emitters have been extensively studied, considering both practical applications as well as geometrical aspects, including shape and positioning of the anode [1–3].

Although the general existing knowledge that the proximity between anode and emitter may affect emission properties, it is found in the literature divergent results on the exact threshold value at which the anode proximity starts to strongly influence the Field Enhancement Factor (hereafter referred as FEF) on the emitter tip [3–5].

In this study we designed a 3D computational model for a single emitter, characterized by the classical hemisphere-on-post geometry, performing extensive parametric simulations in order to investigate electrostatic properties and to understand how the FEF behaves. We also sought to comprehend the setting mechanism of the threshold in which the anode ceases to affect the FEF.

2. Framework

Fig. 1 shows the crosssection of the single emitter in diode configuration. The cold cathode protruding geometry, identified as "emitter", was built by a hemisphere positioned over a cylindrical post – both with radius r. The anode, emitter and substrate structures were kept at constant potentials (Φ) along each step of the simulations, they were also configured as perfect electrical conductors (PEC). Consequently, the Dirichlet boundary condition [6], $\Phi = V_{anode} = 1$ kV could be maintained over the anode surface; the condition $\Phi = 0$ was maintained over the emitter and substrate surfaces. Still in Fig. 1, not only the cylindrical symmetry axis can be noted but also the geometric parameters of the device: r (radius), h (height), G (gap between anode-substrate flat surfaces), $g = G - h$ (gap between the anode and the emitter apex), $AR = h/r$ (emitter aspect ratio), θ (angle between the Z-axis and a point over the emitting surface) and w (radial width of the model). Table 1 correlates the values and respective intervals of each geometric parameter swept with the simulated scenarios.

The width of the model (w) was kept constant at 30 μm for all simulations, permitting the potential distribution (Φ) on the edge of the external sidewall had only variations in the Z direction with a linear trend. This means that the Neumann boundary condition [6] was applied.

We chose to use along this study the Ansys-Maxwell 2015 software, which is a commercially available tool that can perform numerical simulations based on the finite elements method [7]. In 3D models, the tetrahedral elements of the generated mesh are suitable for discretization of steep-angled geometries [8].

Maxwell uses an iterative algorithm to automatically increase the mesh density within regions which show a high field gradient – this technique is referred as adaptive refinement [7]. To guarantee satisfactory convergence and accuracy, the software allows seeding the adaptive refinement through the manual addition of mesh operations and convergence criteria. In field emission

* Corresponding author.

http://dx.doi.org/10.1016/j.ultramic.2015.10.018
0304-3991/

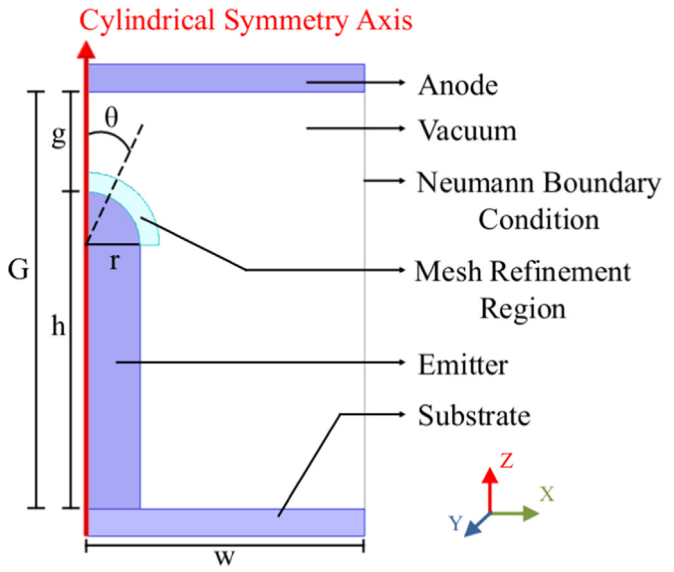

Fig. 1. Cross-sectional view (*not to scale*) of the designed 3D hemisphere-on-post emitter geometry.

Table 1
Parameter values swept along all simulated scenarios.

Fig. no.	r (nm)	h (μm)	$AR=h/r$	G (μm)	θ (deg)
4	10	1	100	10	-
5	10	1	100	100	0–90
6	10	0.01–30	1–3000	100	-
7	5–20	0.005–60	1–3000	100	-
8	5–20	0.5–20	100	See text	-

models the tip region is critical and it requires a highly refined mesh in its surroundings [3,8], thereby extra operations are necessary besides the adaptive refinement.

Considering this, it was created a Mesh Refinement Region (MRR) surrounding the hemispherical surface – see Fig. 1. Such region delimits the effects from the mesh operations and convergence criteria added, consequently minimizing numerical noise and smoothing equipotential lines. The result of the whole refinement process was a highly dense and non-homogeneous mesh in the region of major interest. Fig. 2 shows the generated mesh,

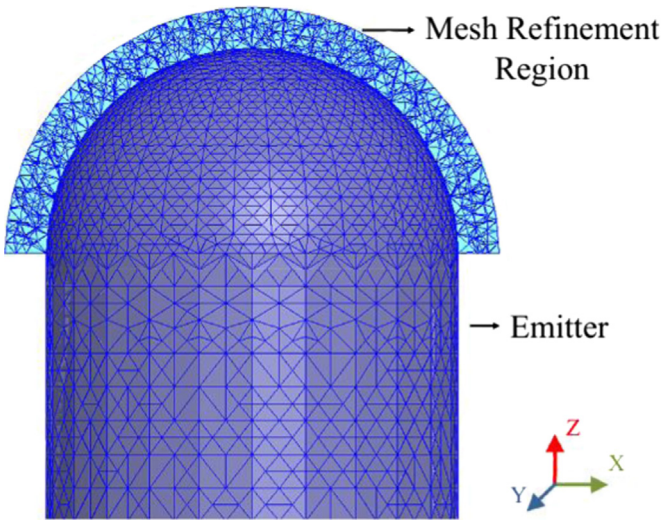

Fig. 2. Non-homogeneous mesh generated at the emitter surface and inside the MRR. Mesh density increases as it approaches the apex.

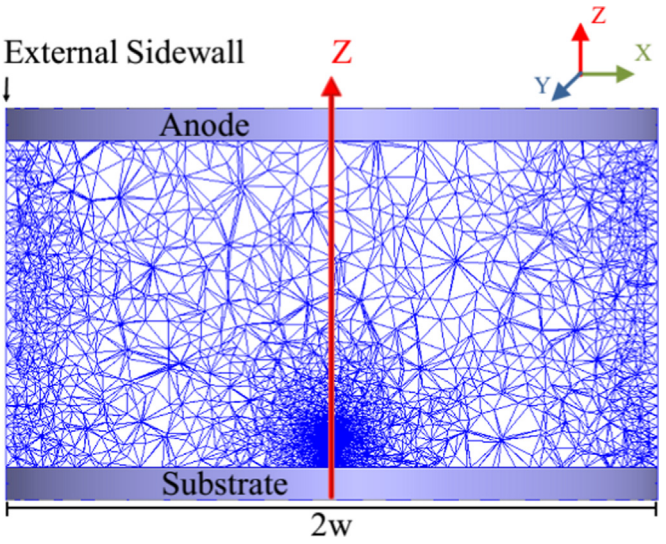

Fig. 3. Cross-sectional view of the entire 3D model showing mesh refinement at the vertical sidewall. In the center, a highly dense mesh can be noted due to the presence of the emitting geometry.

both within the MRR cross section (XZ plane) and over the emitter surface. The MRR thickness was optimized due to project requirements (e.g. accuracy vs. processing time), thus the value of 2 nm was kept constant for all simulations.

Fig. 3 presents a broad visualization of the meshed vacuum region, plotted over the cross section (XZ plane) of the 3D model; the anode, substrate, cylindrical symmetry axis and the external sidewall are also shown. In the central region, a highly dense mesh can be noted due to the emitter and the reasons already mentioned. Additionally, it is possible to observe there was some mesh refinement nearby the sidewalls. Considering both geometric features and biasing excitations, this "vertical refinement" is more efficient than refining its interior (where a coarser mesh can be clearly viewed). This fact is explained by the electromagnetic theory because when a "horizontal refinement" is performed, it unnecessarily increases tetrahedrons over the same equipotential level. This refinement technique contributed to a significant reduction in the percent deviation between results of the present research and from other authors [2,9–11] (detailed in next section).

The electric field intensity within the whole 3D computational domain is obtained through numerical simulations. This implies in the finite elements software solving the Laplace equation. The derivative of the electrostatic potential is calculated at each node of each tetrahedron, considering excitations and boundary conditions previously presented [6,7].

3. Results

The electric field intensity (E) may be represented as in Fig. 4. The spatial distribution of E can be noted in the vacuum region (plotted in the XZ plane) nearby the emitter. The electric field intensity on the emitting surface can be measured through a hemispherical virtual surface, which purpose is to act as probe when involving the original emitting surface. This virtual structure, with infinitesimal thickness, was positioned at 1 nm gap [2] and it did not influence meshing neither the electric field computation. The inset in Fig. 4 shows the scale of E, where a maximum value of approximately 6.5 V/nm can be seen.

In Fig. 5, the electric field intensity is shown as a function of the emitting surface angle in relation to Z-axis, $E(\theta)$. When comparing